ACS APPLIED MATERIALS & INTERFACES

Research Article

www.acsami.org

High-Performance Sensors Based on Resistance Fluctuations of Single-Layer-Graphene Transistors

Kazi Rafsanjani Amin and Aveek Bid*

Department of Physics, Indian Institute of Science, Bangalore, Karnataka, India 560012

ABSTRACT: One of the most interesting predicted applications of graphene-monolayer-based devices is as high-quality sensors. In this article, we show, through systematic experiments, a chemical vapor sensor based on the measurement of low-frequency resistance fluctuations of single-layer-graphene field-effect-transistor devices. The sensor has extremely high sensitivity, very high specificity, high fidelity, and fast response times. The performance of the device using this scheme of measurement (which uses resistance fluctuations as the detection parameter) is more than 2 orders of magnitude better than a detection scheme in which changes in the average value of the resistance is monitored. We propose a number-density-fluctuation-based model to explain the superior characteristics of a noise-measurement-based detection scheme presented in this article.

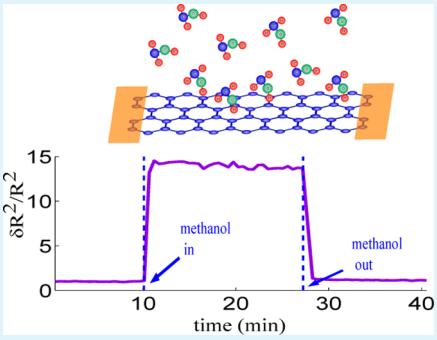

KEYWORDS: *graphene, field-effect transistor, sensor, resistance fluctuations, noise, number-density fluctuation*

1. INTRODUCTION

Single-layer graphene (SLG) has several distinctly unique properties that make it exceptionally suited for use as material and radiation sensors. The specific surface area (2630 $m^2\ g^{-1}$) of SLG is among the highest in layered materials,[1] making the conductance of graphene extremely sensitive to the ambient; that is, the presence of a few foreign molecules on its surface can significantly modify its electrical characteristics. SLG is highly conductive even in very low carrier density regimes, with room temperature mobilities on the order of 20000 $cm^2\ V^{-1}\ s^{-1}$ routinely achievable.[2−4] This causes graphene-based devices to have much lower levels of thermal noise compared to semiconductor-based sensors having comparable carrier densities. The low defect levels of pristine graphene[5−8] ensure that intrinsic flicker noise due to thermal switching of defects is lower than that of any semiconductor material.[9−13] The ability of SLG to interact with materials with a variety of interactions, from weak van der Waals force to extremely stable covalent bonds, raises the possibility of detecting a wide variety of materials with SLG-based sensors with high specificity. Single-layer-graphene field-effect-transistor (SLG-FET) devices thus seem to have almost all of the properties required to be an effective sensor material: accessibility to large surface area, good transduction, electrical and mechanical stability, and ease of preparation.

There have been previous reports of the use of graphene-based sensors to detect various chemical gas molecules like NH_3, CO, NO_2, NO, O_2, CO_2, and H_2,[14,16−21] as well as biomolecules.[23,24] In all of these cases, the change in the resistance of the device was used as the detection parameter. The sensitivity obtained was at best a few percentage points with extremely long device reset times (on the order of tens of minutes to hours), making them unsuitable for any practical applications. This scenario motivates the development of alternate schemes of sensing, which allows fast detection of analytes with similar, if not improved, sensitivity. In a previous publication, we had reported a very high sensitivity of the intrinsic low-frequency resistance noise of SLG-FET devices to the nature of its ambient. We had also elucidated a probable mechanism behind the high sensitivity of the measured noise to changes in the ambient of the graphene device.[25] In this article, we present extensive studies of the sensing of specific gas molecules using resistance fluctuations (noise) of SLG-FET devices. The relative variance $\delta R^2/R^2$ of resistance fluctuations of the devices was found to show reproducible changes upon exposure to many different chemical vapor molecules. The devices had extremely fast response and reset times, on the order of seconds. The sensitivity of the SLG-FET sensor using this technique was more than an order of magnitude better than sensing with the same device using changes in the resistance of the device.

There have been previous demonstrations of the use of resistance fluctuations to detect adsorbed molecules,[26] but a systematic study of the sensitivity, specificity, and response times of the sensors based on this technique is missing. To work as an effective material sensor, a device must satisfy a certain basic set of criterion: (1) it should have a measurable response, (2) the response and reset times must be low, (3) its response must scale as the amount of test molecules in its working range, (4) the response must be reproducible, and (5) there should be selectivity in response to different types of test molecules. We show in this article that SLG-FET using resistance fluctuations as the detection parameter satisfies all of the above criterion extremely well.

Received: July 2, 2015
Accepted: August 24, 2015
Published: August 24, 2015

DOI: 10.1021/acsami.5b05922
ACS Appl. Mater. Interfaces 2015, 7, 19825−19830

2. MEASUREMENT

The devices reported in this article were prepared from natural graphite exfoliated on Si/SiO_2 wafers. Electrical contacts were fabricated using conventional electron-beam lithography,[5] followed by thermal deposition of Cr/Au (5−7 nm/70 nm). Atomic force microscopy and scanning electron microscopy (SEM) were used to determine the surface quality of devices after the lithography processes. Figure 1a shows a false color SEM image of a typical

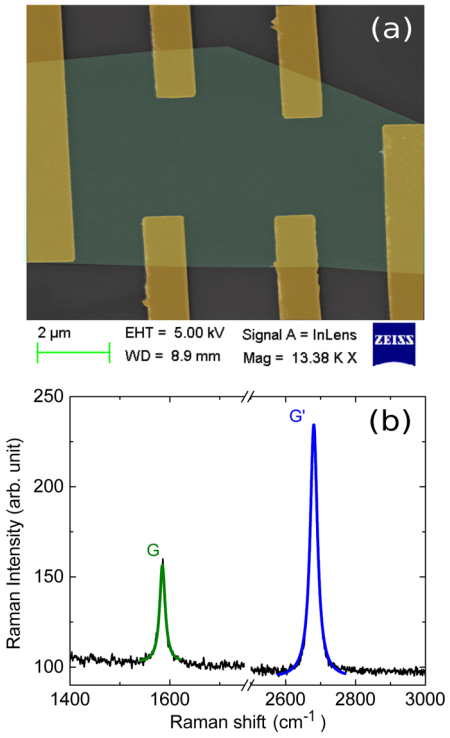

Figure 1. (a) False color SEM image of a typical graphene device. The graphene sheet is shown in light green, and the metal contact pads are shown in yellow. (b) Raman spectrum of the SLG measured after the lithography process. The data are shown as a black line, whereas the green and blue lines are the Lorentzian fits to the G and G′ peaks, respectively.

SLG-FET device. The graphene sheet is shown in light green, and the electrical contact pads are shown in yellow. The number of layers in each device was confirmed through measurement of the Raman spectra of the devices[27−29] and in some cases based on the position of conductance plateaus in the integer quantum hall regime. Figure 1b shows a Raman spectrum of the device: the blue and green lines are the Lorentzian fits to the experimental data. The absence of a D peak, the position of the G peak (1582.2 cm^{-1}), and the ratio of the height of the G peak to that of the G' peak in the Raman spectrum indicate that there is negligible extrinsic doping in the device. Figure 2a shows the gate voltage (V_g) dependence of the resistance from which the mobility (μ) and the impurity charge carrier concentration (n_0) of the device were extracted.[30] Room temperature mobilities of our typical device were in the range of 10000−20000 $cm^2\ V^{-1}\ s^{-1}$, while n_0 was about 10^{12} cm^{-2}. The location of the Dirac point (V_D) very close to zero V_g and the low value of n_0 both attest to the high quality of the devices.

For electrical measurements, the devices were wire-bonded to a lead-less chip carrier and were mounted to a mating socket, which was wired into a custom-built vacuum chamber. The chamber was made of thick stainless steel for better electrical shielding. A schematic diagram of the measurement setup is shown in Figure 3.

The resistance (R) of the graphene FET devices was measured by standard low-frequency alternating-current (ac) lock-in measurement

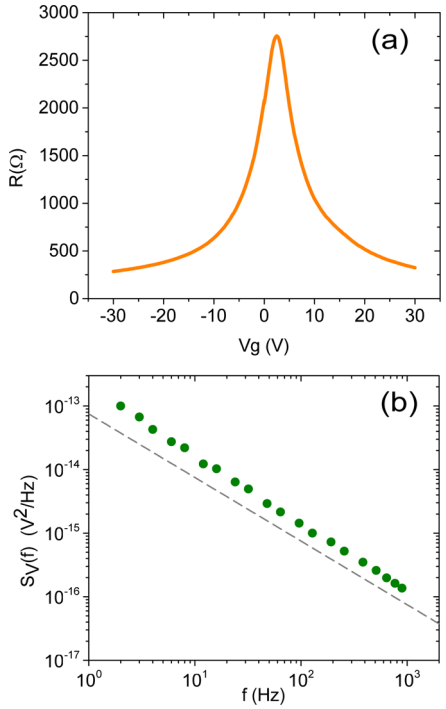

Figure 2. (a) Gate voltage (V_g) dependence on the resistance (R) of an SLG-FET device. (b) Typical $1/f$ noise power spectrum (green filled circles) of a pristine graphene monolayer FET device measured at room temperature. The gray solid line shows a reference $1/f$ curve.

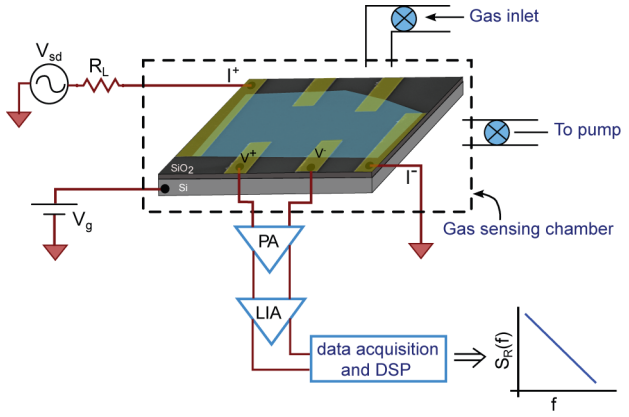

Figure 3. Schematic diagram of the measurement setup. The gas sensing chamber containing the device is shown by the black dotted line. V_{sd} is the ac source−drain bias voltage, R_L is the series ballast resistance (typically about 1 MΩ), and V_g is the direct-current gate bias. PA represents the low-noise preamplifier (SR 552), and LIA is the dual-channel lock-in amplifier (SR 830).

techniques. The power spectral density (PSD) $S_R(f)$ values of low-frequency resistance fluctuations were measured over the frequency bandwidth of 1 Hz to 1 kHz using an ac lock-in detection technique.[31,32] For the measurement of noise, the device was biased with a small ac voltage at a carrier frequency significantly higher than the upper cutoff frequency of the noise measurement bandwidth. The mean four-probe voltage across the device was digitally offset, and the voltage fluctuations $\delta V(t)$ about this mean value were recorded from the output channels of a lock-in amplifier using a high-speed 16-bit digital-to-analog conversion (DAQ) card. The data acquisition rate was determined by the Nyquist criterion, which states that the minimum value of the sampling rate must be at least twice the highest-frequency spectral component present in the signal being studied.[33] The sampling rate was kept usually 8 or 16 times higher than the limit

DOI: 10.1021/acsami.5b05922
ACS Appl. Mater. Interfaces 2015, 7, 19825−19830

given by Nyquist's sampling theorem, and the time series of resistance fluctuations were recorded in contiguous segments of 30 s each. The acquired data were antialiased digitally and down-sampled. The PSD of resistance fluctuations $S_R(f)$ was estimated using Welch's averaged periodogram method.[34] This technique of noise measurement[31,32] allows for a simultaneous measurement of both the intrinsic resistance fluctuations of the device and the background noise arising from thermal fluctuations as well as instrumentation noise. A typical PSD, $S_R(f)$ of resistance fluctuations, of the SLG-FET measured at room temperature is shown in Figure 2b as a function of the frequency f. The resistance fluctuation spectra of pristine graphene devices were always found to be $1/f$ in nature over the entire bandwidth of measurement.

The PSD $S_R(f)$ integrated over the frequency bandwidth of measurement and normalized by the square of the average resistance value gives the relative variance of the resistance fluctuations $\delta R^2/R^2$ (which we refer to as noise):

$$\frac{\delta R^2}{R^2} = \frac{1}{R^2}\int_{f_{min}}^{f_{max}} f S_R(f)\, df \tag{1}$$

Here f_{min} and f_{max} are respectively the lower and upper bounds of the measurement bandwidth.

Graphene has a small but finite work-function difference with metal contact probes, and the fluctuations in the Fermi level near the contact region can generate measurable resistance fluctuations. To address this issue, we have measured $\delta R^2/R^2$ of the device at different applied source−drain voltages V_{sd}. We find that the measured noise always scales with the square of the applied voltage V_{sd} (to within ±5%), showing that the contribution of the contact noise to the observed effect is negligible.[25] As discussed later in this article, we also find that the measured noise has a strong dependence on the gate voltage V_g, suggesting that the major contribution to the measured noise arises from the bulk of the device and not at the contacts.

3. RESULTS AND DISCUSSION

In a typical sensing run, the chamber containing the device was evacuated and the values of both R and $\delta R^2/R^2$ of the device were measured simultaneously to establish the baseline values. The device was then exposed to a known concentration of the chemical for a fixed period of time before the chamber was again evacuated. During this entire process, both the resistance and resistance fluctuations of the device were monitored simultaneously in real time. A typical example of the enhancement in resistance fluctuations of the device upon exposure to chemical vapor is shown in Figure 4a. The blue line shows the resistance fluctuations for the pristine device, while the red line is a plot of the resistance fluctuations after the device has been exposed to 150 ppm of methanol. It can be seen from the time series that upon exposure to methanol the resistance fluctuations of the device are greatly enhanced. Figures 4b and 4c show plots of R and $\delta R^2/R^2$ measured simultaneously during a typical sensing measurement. The values of both parameters have been scaled by their respective values measured in the pristine device. During the first phase of the experiment (region I), the device was maintained in a vacuum and the average R and $\delta R^2/R^2$ values were confirmed to be stable with time. Methanol was introduced into the measurement chamber at the instant of time marked by the black dotted line. It was seen that both R and $\delta R^2/R^2$ increased rapidly before saturation. The change in R was about 6%. On the other hand, the change in $\delta R^2/R^2$ was approximately 1500%, more than 2 orders of magnitude higher than the change in the resistance R. At the end of phase II of the measurement, evacuation of the measurement chamber was started. The resistance takes a long time (on the order of a few

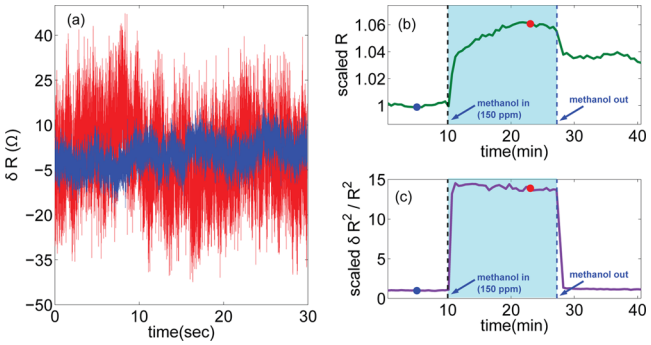

Figure 4. Comparison of the resistance and resistance noise of the SLG-FET device in the absence and presence of analytes. (a) Plot of the time series of resistance fluctuations about the mean value in the pristine SLG-FET device (blue line) and for the same device in the presence of 150 ppm of methanol (red line). It can be seen that the fluctuations in the device resistance are greatly enhanced in the presence of chemical vapor. (b) Plot of scaled R as a function of time for a typical sensing experiment. The resistance changes by about 6% upon exposure to 150 ppm of methanol. (c) Plot of scaled $\delta R^2/R^2$ as a function of time for the same measurement as that in part b. In contrast to R, the noise changes by about 1500% upon exposure to methanol. The blue and red dots represent the points in time when the time series plotted in part a was recorded.

tens of minutes) to go back to its baseline value. This large recovery time of resistance-based graphene sensors was reported earlier by several authors[14,15,18,22,35] and is a major hindrance in implementing resistance-based graphene sensors. On the other hand, the noise $\delta R^2/R^2$ reaches the baseline value within a few seconds. This very fast reset of $\delta R^2/R^2$ holds for a wide range of analyte concentrations and types. Our measurements establish that a chemical sensor based on the resistance fluctuations of the SLG-FET has at least two major advantages over a conventional resistance-based detection scheme: (1) significantly higher sensitivity and (2) a much faster response.

We have shown in a previous publication[25] that that the most probable source of excess noise in these SLG-FET devices upon exposure to analytes is fluctuations in the number density of the charge carriers in the SLG arising from adsorption−desorption of the chemicals at the device surface. The values of the absorption−desorption energy (E_a) for several common analytes on the graphene surface are well-known both from theory and from experiments.[36−41] The presence of a definite energy scale E_a associated with the adsorption−desorption of a specific gas on the graphene surface gives rise to a characteristic frequency scale f_C in the measured $1/f$ noise spectrum. This characteristic frequency f_C is directly related the absorption−desorption activation energy E_a through the equation

$$f_C = f_0 \exp\left[\frac{-E_a(T)}{k_B T}\right] \tag{2}$$

where f_0 is the attempt frequency for the thermally activated process.[25,35] The presence of a characteristic frequency f_C in the measured $1/f$ spectrum is thus a spectroscopic signature specific to the analyte and allows detection with specificity even in the presence of a mixture of gases.[25]

Intuitively, it appears that the sensing efficiency should be strongly correlated to the number density and to the nature of the charge carriers present in the SLG. To test this, we have carried out the sensing measurements at different values of back gate voltage (V_g); the results for a typical measurement are

DOI: 10.1021/acsami.5b05922
ACS Appl. Mater. Interfaces 2015, 7, 19825−19830

plotted in Figure 5a. The green open circles are the relative variance $\delta R^2/R^2$ measured before the sensing experiment. The

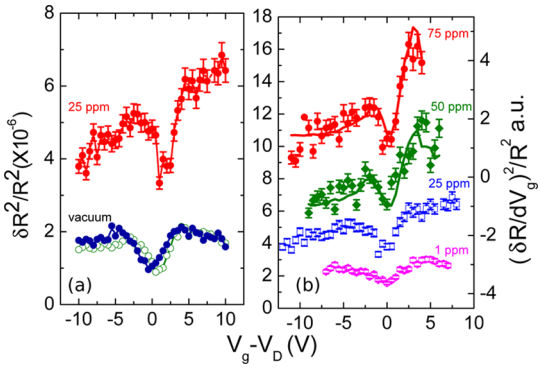

Figure 5. (a) Plots of $\delta R^2/R^2$ as a function of the reduced gate voltage ($V_g - V_D$) of the pristine SLG-FET device (green open circles), after the introduction of 25 ppm of methanol to the measurement chamber (red filled circles) and after the methanol vapor has been pumped out (blue filled circles). (b) Plots of $\delta R^2/R^2$ as a function of the reduced gate voltage ($V_g - V_D$) after the SLG-FET has been exposed to different amounts of methanol vapor: 1 ppm (magenta open circles); 25 ppm (blue open squares); 50 ppm (green filled diamonds); 75 ppm (red filled circles). (right axis) Plot of $1/R\ (dR/dV_g)^2$ for 50 ppm of methanol (green line) and 75 ppm of methanol (red line).

noise as a function of V_g has the symmetric M shape typical of high-quality SLG devices. After each measurement, the measurement chamber was pumped out and the noise measured *again* as a function of the gate voltage. It was seen that the noise in the device after the analyte was pumped out always came back to the baseline value of the pristine SLG-FET, as shown by the blue filled circles in Figure 5a.

The red curve represents the noise $\delta R^2/R^2$ measured after the device has been exposed to 25 ppm of methanol. We note that there are two important features of the graph. First, the noise is greatly enhanced at all values of V_g in comparison to that in the pristine device. The second interesting feature is that the measured noise is no longer symmetric about the Dirac point; for a given amount of a certain analyte, the measured noise was seen to increase as the gate voltage was progressively made positive. In other words, the response of the graphene monolayer, when exposed to a fixed amount of analyte, was not symmetric in the electron- and hole-doped regimes; the response was much stronger in the electron-doped regime ($V_g - V_D > 0$) than in the hole-doped regime ($V_g - V_D < 0$). The slope of the noise plots as a function of the gate voltage at high values of $|V_g - V_D|$, where V_D is the Dirac point of graphene, was seen to scale almost linearly with the amount of analyte. This can be seen clearly in Figure 5b, where we plot the noise as a function of V_g in the presence of various concentrations of methanol. The evolution of the shape of the noise plots as a function of V_g for different levels of exposure to the analyte can be explained using the following analysis: if the dominant source of resistance noise in these devices upon exposure to the analyte is fluctuations in the number density n of charge carriers in the conducting channel, then the following relation holds: $\delta R = (\delta R/\delta n)\ \delta n$. Because the carrier concentration is controlled by the back gate voltage V_g, the contribution to the resistance noise from number-density fluctuations would be $\delta R^2/R^2 \propto (dR/dV_g)^2/R^2$.[12] The values of $(dR/dV_g)^2/R^2$ calculated from the measured $R-V_g$ curves are plotted on the right axis in Figure 5b. There is a very good qualitative match between the experimental data and calculated plots. This shows that for the SLG-FET devices exposed to chemicals number-density fluctuations are most probably the primary source of resistance fluctuation noise.

To test the scaling of the response of the SLG sensor with the concentration of the analytes, measurements similar to those described above were performed by exposing the SLG-FET sensor to different amounts of chemicals. The results obtained for methanol vapor ranging in concentration from 20 to 300 ppm are summarized in Figure 6. Figure 6a shows the

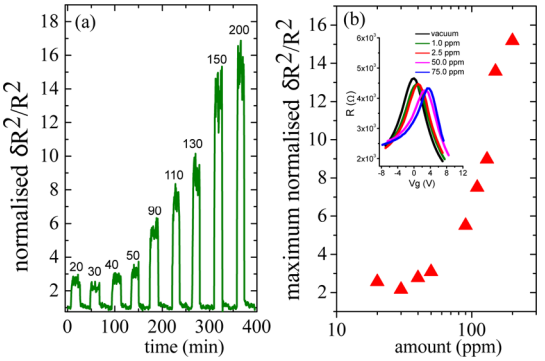

Figure 6. (a) Plot of the relative variance $\delta R^2/R^2$ of the SLG-FET device when exposed to different amounts of methanol vapor ranging from 20 to 200 ppm. Very small response and reset times were observed in all cases. (b) Plot of the average saturation value of $\delta R^2/R^2$ in the presence of different concentrations of methanol vapor. The data have been normalized by the baseline value of $\delta R^2/R^2$ before exposure to methanol. Inset: $R-V_g$ plots measured in the presence of different amounts of methanol vapor.

$\delta R^2/R^2$ values with time for consecutive measurements carried out with different concentrations of methanol vapor. In the plot, the values of $\delta R^2/R^2$ have been scaled by the baseline value of $\delta R^2/R^2$ measured in the pristine SLG device. Note that in each case the value of the relative variance $\delta R^2/R^2$ resets to the initial state as the methanol vapor is pumped out. The average increase in $\delta R^2/R^2$ after the device had been exposed to methanol normalized by the baseline value of $\delta R^2/R^2$ is plotted in Figure 6b. The relative variance of resistance fluctuations $\delta R^2/R^2$ was found to increase with the amount of analyte present in the measurement chamber; this scaling behavior was reproducible over several devices.

To test the reproducibility of our sensing scheme with noise, the SLG device was exposed to the same amount of methanol multiple times. After each exposure, the device chamber was evacuated and it was ensured that the noise went down to the baseline value. A representative result is shown in Figure 7, where the normalized $\delta R^2/R^2$ is plotted as a function of time. From the plot, it can be seen that every time the device was exposed to 100 ppm of methanol vapor the relative variance of resistance fluctuations $\delta R^2/R^2$ scaled up to the same average value, and upon pumping, it sharply reset to the initial state. For detection of 100 ppm of methanol, the observed spread in the average value corresponds to an error in the detection of 0.20 ppm, attesting to the high fidelity of the sensor response.

Our sensing scheme based on noise measurements was tested using different types of molecules. The qualitative trend of fast response and high sensitivity was observed for all of the chemicals tested. The quantitative response of $\delta R^2/R^2$ to vapors of different chemicals varied, ranging from a ~70% change for chloroform to a ~300% change in the case of nitrobenzene. In

DOI: 10.1021/acsami.5b05922
ACS Appl. Mater. Interfaces 2015, 7, 19825−19830

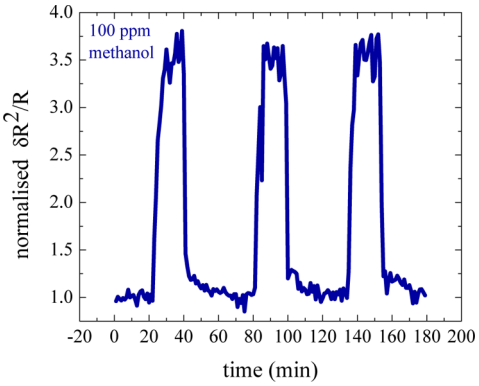

Figure 7. Plot showing the reproducibility in the change of $\delta R^2/R^2$ of the SLG device for three consecutive runs with 100 ppm of methanol.

Figure 8, we plot the response of the SLG sensor exposed to 100 ppm vapors of methanol, ammonia, chloroform, and

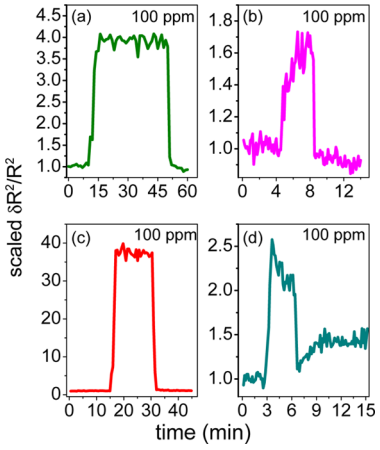

Figure 8. Plots of $\delta R^2/R^2$ during sensing experiments with the SLG-FET device exposed to 100 ppm of different chemicals: (a) methanol; (b) chloroform; (c) nitrobenzene; (d) ammonia.

nitrobenzene. We were especially interested in the detection of nitrobenzene because nitro group chemicals are extensively used in explosives. In our measurements, $\delta R^2/R^2$ in the graphene device was observed to be highly sensitive to the presence of nitrobenzene even at very low concentration, making it a very promising sensor for the detection of explosives.

We currently do not have a clear understanding of the strong response of the SLG-FET sensor to nitrobenzene. It has been predicted that the NO_2 functional group associated with nitrobenzene has a very strong affinity with graphene, which can result in strong scattering centers. A dynamic fluctuation of a strong scattering potential, resulting from the absorption−desprption of nitrobenzene, might lead to the high noise levels measured. We believe that further experimental and theoretical work is needed to address this issue.

4. CONCLUSION

In conclusion, we present experiments testing the efficacy of graphene-monolayer FET-based devices as chemical sensors. We find that a detection scheme based on measurements of the resistance fluctuations is far superior to the traditional method of measuring the average resistance change in terms of the sensitivity, specificity, and response time of the detector. We show that, for monolayer graphene devices exposed to the ambient, the most likely source of enhanced resistance fluctuations is fluctuation in the carrier number density. To the best of our knowledge, graphene-based chemical sensors with these characteristics have not been reported before.

AUTHOR INFORMATION

Corresponding Author

*E-mail: aveek.bid@physics.iisc.ernet.in.

Notes

The authors declare no competing financial interest.

ACKNOWLEDGMENTS

The authors thank the NPMASS, Government of India, for support. The authors thank device fabrication and characterization facilities at the National Nanofabrication Centre and Micro and Nano Characterization Facility in the Centre for Nano Science and Engineering at IISc, Bangalore. K.R.A. thanks the CSIR, MHRDG, Government of India, for support.

REFERENCES

(1) Pumera, M.; Ambrosi, A.; Bonanni, A.; Chng, E. L. K.; Poh, H. L. Graphene for Electrochemical Sensing and Biosensing. *TrAC, Trends Anal. Chem.* **2010**, *29*, 954−965.
(2) Soldano, C.; Mahmood, A.; Dujardin, E. Production, Properties and Potential of Graphene. *Carbon* **2010**, *48*, 2127−2150.
(3) Zheng, M.; Takei, K.; Hsia, B.; Fang, H.; Zhang, X.; Ferralis, N.; Ko, H.; Chueh, Y.-L.; Zhang, Y.; Maboudian, R.; Javey, A. Metal-catalyzed Crystallization of Amorphous Carbon to Graphene. *Appl. Phys. Lett.* **2010**, *96*, 063110.
(4) Abergel, D. S. L.; Apalkov, V.; Berashevich, J.; Ziegler, K.; Chakraborty, T. Properties of Graphene: a Theoretical perspective. *Adv. Phys.* **2010**, *59*, 261−482.
(5) Novoselov, K. S.; Geim, A. K.; Morozov, S. V.; Jiang, D.; Zhang, Y.; Dubonos, S. V.; Grigorieva, I. V.; Firsov, A. A. Electric Field Effect in Atomically Thin Carbon Films. *Science* **2004**, *306*, 666−669.
(6) PMID 18298094: Lin, Y.-M.; Avouris, P. Strong Suppression of Electrical Noise in Bilayer Graphene Nanodevices. *Nano Lett.* **2008**, *8*, 2119−2125.
(7) Ratinac, K. R.; Yang, W.; Ringer, S. P.; Braet, F. Toward Ubiquitous Environmental Gas Sensors - Capitalizing on the Promise of Graphene. *Environ. Sci. Technol.* **2010**, *44*, 1167−1176.
(8) Shao, Q.; Liu, G.; Teweldebrhan, D.; Balandin, A. A.; Rumyantsev, S.; Shur, M.; Yan, D. Flicker Noise in Bilayer Graphene Transistors. *IEEE Electron Device Lett.* **2009**, *30*, 288−290.
(9) Balandin, A. A. Low-frequency 1/f Noise in Graphene Devices. *Nat. Nanotechnol.* **2013**, *8*, 549−555.
(10) Xu, G.; Torres, C. M., Jr; Zhang, Y.; Liu, F.; Song, E. B.; Wang, M.; Zhou, Y.; Zeng, C.; Wang, K. L. Effect of Spatial Charge Inhomogeneity on 1/f Noise Behavior in Graphene. *Nano Lett.* **2010**, *10*, 3312−3317.
(11) Pal, A. N.; Ghatak, S.; Kochat, V.; Sneha, E.; Sampathkumar, A.; Raghavan, S.; Ghosh, A. Microscopic Mechanism of 1/f Noise in Graphene: Role of Energy Band Dispersion. *ACS Nano* **2011**, *5*, 2075−2081.
(12) Kaverzin, A.; Mayorov, A. S.; Shytov, A.; Horsell, D. Impurities as a Source of 1/f Noise in Graphene. *Phys. Rev. B: Condens. Matter Mater. Phys.* **2012**, *85*, 075435.
(13) Pellegrini, B. 1/f Noise in Graphene. *Eur. Phys. J. B* **2013**, *86*, 1−12.
(14) Schedin, F.; Geim, A.; Morozov, S.; Hill, E.; Blake, P.; Katsnelson, M.; Novoselov, K. Detection of Individual Gas Molecules Adsorbed on Graphene. *Nat. Mater.* **2007**, *6*, 652−655.
(15) Chen, G.; Paronyan, T. M.; Harutyunyan, A. R. Sub-ppt Gas Detection with Pristine Graphene. *Appl. Phys. Lett.* **2012**, *101*, 053119.

DOI: 10.1021/acsami.5b05922
ACS Appl. Mater. Interfaces 2015, 7, 19825−19830

(16) Chen, C. W.; Hung, S. C.; Yang, M. D.; Yeh, C. W.; Wu, C. H.; Chi, G. C.; Ren, F.; Pearton, S. J. Oxygen Sensors made by Monolayer Graphene under Room Temperature. *Appl. Phys. Lett.* **2011**, *99*, 243502.
(17) Yoon, H. J.; Jun, D. H.; Yang, J. H.; Zhou, Z.; Yang, S. S.; Cheng, M. M.-C. Carbon dioxide Gas Sensor using a Graphene Sheet. *Sens. Actuators, B* **2011**, *157*, 310−313.
(18) Wu, W.; Liu, Z.; Jauregui, L. A.; Yu, Q.; Pillai, R.; Cao, H.; Bao, J.; Chen, Y. P.; Pei, S.-S. Wafer-scale Synthesis of Graphene by Chemical Vapor Deposition and its Application in Hydrogen Sensing. *Sens. Actuators, B* **2010**, *150*, 296−300.
(19) Amin, K. R.; Bid, A. Graphene as a Sensor. *Curr. Sci.* **2014**, *107*, 430−436.
(20) Yavari, F.; Koratkar, N. Graphene-based Chemical Sensors. *J. Phys. Chem. Lett.* **2012**, *3*, 1746−1753.
(21) Yuan, W.; Shi, G. Graphene-based Gas Sensors. *J. Mater. Chem. A* **2013**, *1*, 10078−10091.
(22) Iezhokin, I.; Offermans, P.; Brongersma, S. H.; Giesbers, A. J. M.; Flipse, C. F. J. High Sensitive Quasi Freestanding Epitaxial Graphene Gas Sensor on 6H-SiC. *Appl. Phys. Lett.* **2013**, *103*, 053514.
(23) Dong, X.; Shi, Y.; Huang, W.; Chen, P.; Li, L.-J. Electrical Detection of DNA Hybridization with Single-Base Specificity Using Transistors Based on CVD-Grown Graphene Sheets. *Adv. Mater. (Weinheim, Ger.)* **2010**, *22*, 1649−1653.
(24) Dong, X.; Huang, W.; Chen, P. In situ Synthesis of Reduced Graphene Oxide and Gold Nanocomposites for Nanoelectronics and Biosensing. *Nanoscale Res. Lett.* **2010**, *6*, 60.
(25) Amin, K. R.; Bid, A. Effect of Ambient on the Resistance Fluctuations of Graphene. *Appl. Phys. Lett.* **2015**, *106*, 183105.
(26) Rumyantsev, S.; Liu, G.; Shur, M. S.; Potyrailo, R. A.; Balandin, A. A. Selective Gas Sensing with a Single Pristine Graphene Transistor. *Nano Lett.* **2012**, *12*, 2294−2298.
(27) Ferrari, A. C.; Meyer, J. C.; Scardaci, V.; Casiraghi, C.; Lazzeri, M.; Mauri, F.; Piscanec, S.; Jiang, D.; Novoselov, K. S.; Roth, S.; Geim, A. K. Raman Spectrum of Graphene and Graphene Layers. *Phys. Rev. Lett.* **2006**, *97*, 187401.
(28) Ferrari, A. C. Raman Spectroscopy of Graphene and Graphite: Disorder, Electron-Phonon Coupling, Doping and Nonadiabatic effects. *Solid State Commun.* **2007**, *143*, 47−57.
(29) Malard, L. M.; Pimenta, M. A.; Dresselhaus, G.; Dresselhaus, M. S. Raman Spectroscopy in Graphene. *Phys. Rep.* **2009**, *473*, 51.
(30) Zhu, W.; Perebeinos, V.; Freitag, M.; Avouris, P. Carrier Scattering, Mobilities, and Electrostatic Potential in Monolayer, Bilayer, and Trilayer Graphene. *Phys. Rev. B: Condens. Matter Mater. Phys.* **2009**, *80*, 235402.
(31) Ghosh, A.; Kar, S.; Bid, A.; Raychaudhuri, A. A set-up for Measurement of Low Frequency Conductance Fluctuation (Noise) using Digital Signal Processing techniques. *arXiv.org, e-Print Arch., Condens. Matter* **2004**.
(32) Scofield, J. H. ac Method for Measuring Low-frequency Resistance Fluctuation Spectra. *Rev. Sci. Instrum.* **1987**, *58*, 985−993.
(33) Shannon, C. E. Communication in the Presence of Noise. *Proc. IRE* **1949**, *37*, 10−21.
(34) Welch, P. D. The use of Fast Fourier Transform for the Estimation of Power Spectra: A Method based on Time Averaging over Short, Modified Periodograms. *IEEE Trans. Audio Electroacoust.* **1967**, *15*, 70−73.
(35) Rumyantsev, S.; Liu, G.; Potyrailo, R.; Balandin, A.; Shur, M. Selective Sensing of Individual Gases Using Graphene Devices. *IEEE Sens. J.* **2013**, *13*, 2818−2822.
(36) Pankewitz, T.; Klopper, W. *Ab Initio* Modeling of Methanol Interaction with Single-Walled Carbon Nanotubes. *J. Phys. Chem. C* **2007**, *111*, 18917−18926.
(37) Gautam, M.; Jayatissa, A. H. Graphene based Field Effect Transistor for the Detection of Ammonia. *J. Appl. Phys.* **2012**, *112*, 064304.
(38) Akesson, J.; Sundborg, O.; Wahlstrom, O.; Schroder, E. A van der Waals Density Functional study of Chloroform and other Trihalomethanes on Graphene. *J. Chem. Phys.* **2012**, *137*, 174702.
(39) Lazar, P.; Karlicky, F.; Jurecka, P.; Kocman, M.; Otyepkova, E.; Safarova, K.; Otyepka, M. Adsorption of Small Organic Molecules on Graphene. *J. Am. Chem. Soc.* **2013**, *135*, 6372−6377.
(40) Lin, X.; Ni, J.; Fang, C. Adsorption Capacity of H2O, NH3, CO, and NO2 on the Pristine Graphene. *J. Appl. Phys.* **2013**, *113*, 034306.
(41) Huang, B.; Li, Z.; Liu, Z.; Zhou, G.; Hao, S.; Wu, J.; Gu, B.-L.; Duan, W. Adsorption of Gas Molecules on Graphene Nanoribbons and Its Implication for Nanoscale Molecule Sensor. *J. Phys. Chem. C* **2008**, *112*, 13442−13446.

DOI: 10.1021/acsami.5b05922
ACS Appl. Mater. Interfaces 2015, 7, 19825−19830